J-matrix calculation of electron-helium S-wave scattering. II. Beyond the frozen-core model

Dmitry A. Konovalov
ARC Centre for Antimatter-Matter Studies and Discipline of Information Technology, School of Business, James Cook University, Townsville, Queensland 4811, Australia

Dmitry V. Fursa and Igor Bray
ARC Centre for Antimatter-Matter Studies, Curtin University, GPO Box U1987, Perth, Western Australia 6845, Australia

(Dated: September 3, 2012)

In the preceding J-matrix (JM) paper [D. A. Konovalov *et. al.* Phys. Rev. A **84**, 032707 (2011)], the S-wave e-He scattering (S-e-He) problem was solved within the frozen-core (FC) model of helium for impact energies in the range 0.1-1000eV. In this sequel, both target electrons are described within the configuration-interaction model of helium obtaining more accurate (compared to the FC model) first seven bound states of the S-wave helium. The presented JM calculations solve the S-e-He problem essentially exactly for the total elastic, $2^{1,3}S$, $3^{1,3}S$ excitation cross sections below the ionization threshold. The JM results are confirmed by the corresponding convergent-close-coupling (CCC) calculations creating a challenging benchmark for any current or future *ab initio* electron-atom scattering methods.

Above the ionization threshold, only the elastic and triplet 2^3S excitation cross sections are obtained at the benchmark accuracy level. The total ionization and the rest of excitation cross sections still exhibit noticeable pseudo-resonances (up to 10% fluctuations), which could not be eliminated with the considered number of target states (up to 95 eigenstates of He were considered).

PACS numbers: 34.80.Dp

I. INTRODUCTION

This study focuses on the S-wave e-He (S-e-He) scattering, where the target helium atom is in its ground state before the electron impact, and where only the partial wave with zero angular momentum ($l = 0$) is retained in all calculations and partial-wave expansions. The S-wave models have proven to be a very productive testing ground for *ab initio* scattering theories, see [1–18] for the S-wave e-H scattering (S-e-H) and [19–27] for the S-e-He problem. The main attraction of the S-wave models is that they retain most of the physics complexities of the full scattering problems while reduce the problems computationally. In particular, it is somewhat expected and implied that if a theoretical method solves a S-wave model, then the remaining partial waves could be solved with additional computational resources, which is indeed the case for the convergent-close-coupling (CCC) [28], R-matrix (RM) [29, 30] and J-matrix (JM) [31, 32] methods.

The main goal of this study is to provide high accuracy total elastic and excitation S-e-He cross sections for 5-100eV impact energies highlighting resonant features of the cross sections. The need for such benchmark theoretical data is evident from the existing *ab initio* attempts to solve the S-e-He problem. Reviewing in reverse chronological order, in 2010, Bartlett and Stelbovics [25] developed a four-body propagating exterior scaling (PECS) method and reported results claiming to achieve "benchmark" level of accuracy. However none of their cross sections, including elastic and $2^{1,3}S$ excitation cross sections, displayed any resonances at the accuracy level achieved for the S-e-H problem [3]. In 2005, Horner et al. [24] reported results using time-dependent exterior complex scaling (TD-ECS), which also failed to described resonance behavior of the cross sections. In 2002 and 2004, the CCC method [21, 22] also did not examine the resonance regions with sufficiently fine energy grid. This is now corrected to some extent when in 2011 Konovalov et al. [27] reported the CCC and JM *frozen-core* (FC) results clearly showing the resonances in the elastic and $n = 2$ (2^1S and 2^3S) excitation cross sections. And finally, the RM method [29, 30] has never reported its results for the S-e-He problem.

The stated goal is attempted and achieved in many aspects by combining advantages of the CCC and JM methods, where the later has been recently revised [27] by merging it with the Fano's multi-configuration interaction matrix elements [33]. The CCC method is able to solve the scattering problem very accurately via the Lippmann-Schwinger equation [34]. However, it is not practical to run the CCC method for each of the many thousands of impact energy points required for the final benchmark results. On the other hand, the JM method is very efficient [35, 36] in calculating a vast number of energy points but numerical-convergence properties of the JM method remains largely unknown. The JM and CCC methods are implemented independently and use completely different approaches to solve the scattering equations. Therefore, the CCC and JM methods can be and

were used to cross-verify that their results are convergent within their own numerical parameters at key energy points.

The presented JM method is implemented using Java programming language, which is freely available for MS Windows, Mac OS, and many versions of Linux or Unix. See [37] for information on availability of the results and source code.

TABLE I: Energies and classifications for S-wave helium electron configurations. $\lambda_c = 4$, $\lambda_t = 1$, a.u.= 27.2116eV

Classification	threshold [eV]	Eigenvalues [a.u]	(N_c,N_t)
He$(1s^2,^1S)$	0	-2.879 028 569 1	(50,50)
error =	0.001 80	-2.878 962 303	(7,30)
error =	0.177 47	-2.872 506 673	(1,30)
He$(1s2s,^3S)$	19.178	-2.174 264 856 3	(50,50)
		-2.174 264 618	(7,30)
		-2.174 245 504	(1,30)
He$(1s2s,^1S)$	19.996	-2.144 197 258 7	(50,50)
		-2.144 191 393	(7,30)
		-2.143 449 321	(1,30)
He$(1s3s,^3S)$	22.056	-2.068 490 070	(7,30)
		-2.068 484 660	(1,30)
He$(1s3s,^1S)$	22.266	-2.060 792 356	(7,30)
		-2.060 573 161	(1,30)
He$(1s4s,^3S)$	22.928	-2.036 438 560	(7,30)
		-2.036 436 372	(1,30)
He$(1s4s,^1S)$	23.011	-2.033 392 203	(7,30)
		-2.033 300 706	(1,30)
He$(1s5s,^3S)$	23.305	-2.022 583 695	(7,30)
		-2.022 582 608	(1,30)
He$(1s5s,^1S)$	23.346	-2.021 079 423	(7,30)
		-2.021 033 007	(1,30)
$He^+(1s)$	23.920	-2	Ionization

II. THEORY

The JM method [35, 36] is a very general method for solving wide range of scattering problems. In this study, we continue to develop the version of the JM method that was previously applied to the S-e-H [38] and S-e-He [27] scattering problems. Hereafter this version will be referred to as the KFB method to assist when discussing its features which are not part of the generic JM method.

When the KFB method was applied to the FC model of helium [27] (one electron was always in the $1s$ state of He^+), the following three sets of functions were used: target basis, JM functions, and Laguerre basis.

Target basis is a set of N_t orthonormal radial functions $\{P_n(r)\}_{n=1}^{N_t}$, where $P_n(r)$ is used as the radial component of the n'th subshell wave function when building one- or many-electron wave functions as per the Fano's procedure [27, 33].

JM functions are the nonorthogonal Laguerre functions $\{\xi_p(r)\}_{p=0}^{\infty}$ from the original JM method [35, 36],

$$\xi_p(r) = x^{l+1}\mathrm{e}^{-x/2}L_p^{2l+1}(x), \quad p = 0, 1, ..., \infty, \quad (1)$$

where $x = \lambda r$, λ is Laguerre exponential falloff, $l \equiv 0$ (for the S-model), and $L_p^{\alpha}(x)$ are the associated Laguerre polynomials [39].

Laguerre basis is the set of orthonormal Laguerre functions $\{R_p(r)\}_{p=0}^{\infty}$,

$$R_p(r) = C_p x^{l+1}\mathrm{e}^{-x/2}L_p^{2l+2}(x), \quad p = 0, 1, ..., \infty, \quad (2)$$

$$\int_0^{\infty} dr\ R_p(r)R_{p'}(r) = \delta_{pp'},\ C_p = \sqrt{\frac{\lambda p!}{(p+2l+2)!}}. \quad (3)$$

Note that for any fixed N_t, both $\{\xi_p(r)\}_{p=0}^{N_t}$ and $\{R_p(r)\}_{p=0}^{N_t}$ span identical functional space [38].

The target basis $\{P_n(r)\}_{n=1}^{N_t}$ is selected or built by diagonalizing a suitable one-electron Hamiltonian [27, 38]. Then, the two-electron target-helium wave functions are constructed by allowing first and second helium electrons to occupy the first N_c and N_t radial functions, respectively, where N_c controls the number of allowed *core* excitations with $N_c = 1$ being the frozen-core model. After many numerical experiments, it became apparent that the core excitation functions $\{P_n(r)\}_{n=1}^{N_c}$ should be constructed differently from the rest of the target basis $\{P_n(r)\}_{n=N_c+1}^{N_t}$. Otherwise, the convergence by N_c is just too slow to be computationally practical. This is due to the two very different radial scales present in this study. The short-range core excitations are essentially adjustments to the $1s$-orbital of He^+. While the He excitations (below the ionization threshold) resemble ns-orbitals of hydrogen and therefore are long-range. This problem is solved here by using a mix of the short range $\{R_p^c(r)\}_{p=0}^{N_c-1}$ with $\lambda_c = 4$ and long-range $\{R_p^t(r)\}_{p=N_c}^{N_t-1}$ with $\lambda_t = 1$ basis sets when constructing the target basis as follows.

The JM method splits the one-electron radial functional space into *inner* $\{\xi_p\}_{p=0}^{N-1}$ and *outer* $\{\xi_p\}_{p=N}^{\infty}$ subsets controlled by the number N of JM functions in the inner subset [35, 36]. In the KFB method, the target basis $\{P_n(r)\}_{n=1}^{N_t}$ must be orthogonal to the outer JM functions $\{\xi_p\}_{p=N}^{\infty}$, where $N_t < N$. Let $\lambda \equiv \lambda_t$ and $\hat{I}_t$ be a projection operator into the functional space of $\{R_p^t(r)\}_{p=0}^{N_t-1}$

$$\hat{I}_t = \sum_{p=0}^{N_t-1} |R_p^t\rangle\langle R_p^t|, \quad (4)$$

then by construction every function from $\{R_p^t(r)\}_{p=0}^{N_t-1}$ and $\{R_p^{ct}(r)\}_{p=0}^{N_c-1}$

$$R_p^{ct} = \hat{I}_t R_p^c, \quad (5)$$

is orthogonal the outer JM functions. Then the final target basis $\{P_n(r)\}_{n=1}^{N_t}$ is constructed by making a single

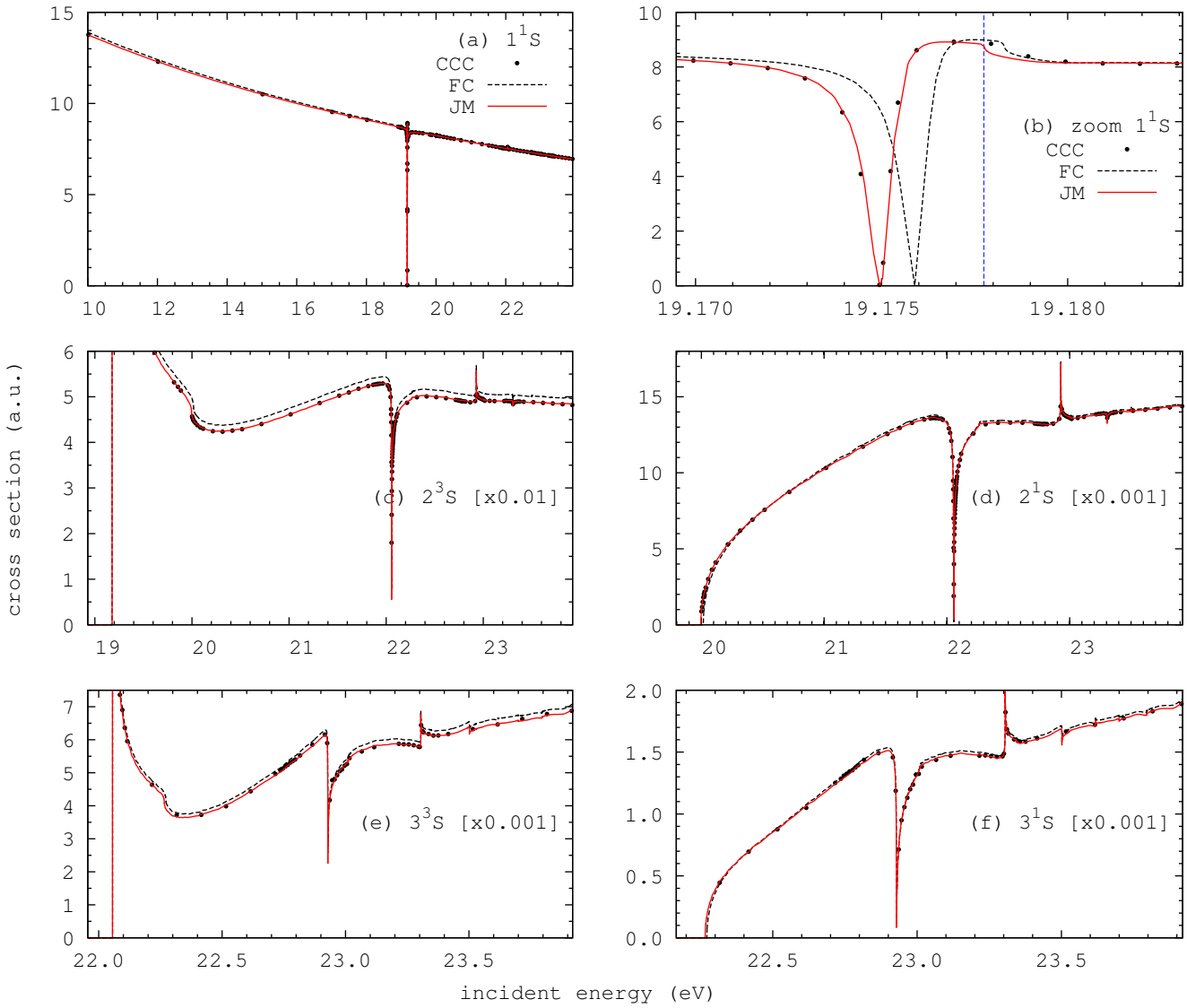

FIG. 1: (Color online) Elastic (1^1S), $n = 2$ (2^3S and 2^1S) and $n = 3$ (3^3S and 3^1S) single-excitation cross sections below the ionization threshold (23.92eV from Table I) for the e-He S-wave scattering model. Sub-figure (b) zooms in on the 2^3S excitation threshold (Table I) shown by the vertical dashed line. Frozen-core (FC), JM and CCC results were shifted by 0.17747eV, 0.0018eV and 0.0018eV (Table I), respectively.

orthonormal basis from $\{R^{ct}_p(r)\}_{p=0}^{N_c-1}$ and $\{R^{t}_p(r)\}_{p=N_c}^{N_t-1}$ via the Gram-Schmidt process.

Note that in the CCC method the final target basis $\{P^{3C}_n(r)\}_{n=1}^{N_t}$ is also built via the Gram-Schmidt process but from $\{R^{c}_p(r)\}_{p=0}^{N_c-1}$ and $\{R^{t}_p(r)\}_{p=N_c}^{N_t-1}$ sets, that is, the R^{ct}_p functions were not required.

The number N is the key JM parameter responsible for the convergence of any implementation of the JM method. That is, the larger the N, the more accurate the corresponding JM results are expected to be. Within the current KFB method, maximum value of N is limited to around 100 so that the method remains to be easily accessible to wider research community. All presented in this study KFB results were still calculated on a consumer-grade laptop.

III. RESULTS

The following KFB computational parameters were used, see [38] for explanation of the parameters: $\lambda_c = 4$, $\lambda_t = 1$, $N_t = 30$, $N = 10$, $\ln(c) = -5-2\ln(Z_{\rm He})$, $Z_{\rm He} = 2$, $r_{\rm max} = 500$, $M_{LCR} = 2001$, where the radial grid was between zero and $r_{\rm max}$ and M_{LCR} is the number of equally spaced points in the radial LCR grid [38]. When converting to eV scale, 27.2116 eV was used as the atomic unit of energy (or Hartree).

TODO: A tabular form of the JM and CCC cross sec-

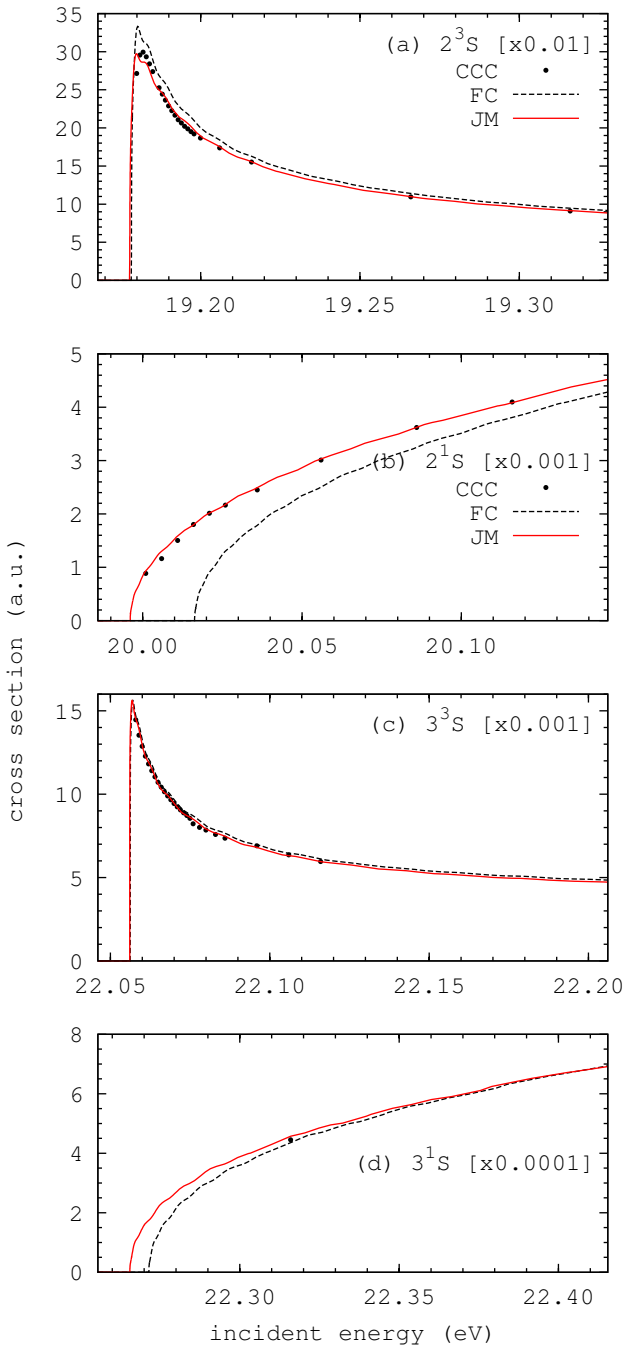

FIG. 2: (Color online) The same as in Fig. 1 but zooming in on the corresponding excitation threshold energies (Table I).

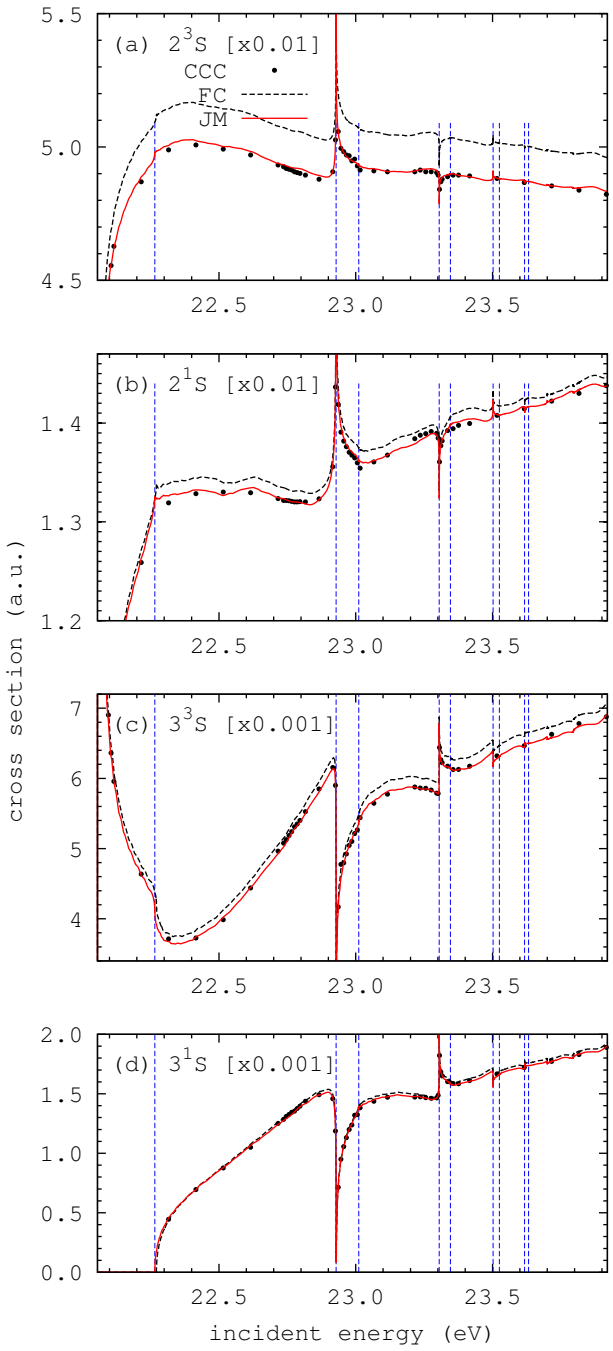

FIG. 3: (Color online) The same as in Fig. 1 but starting from the 3^3S threshold and aligned by incident energies. The 3^1S, $4^{3,1}S$, ..., $7^{3,1}S$, excitation thresholds (Table I) are shown by vertical dashed lines (from left to right).

tions is available from jmatrix.googlecode.com CHECK PhysRev email on how to upload data to them.

IV. CONCLUSIONS

Acknowledgments

This work was supported by the Australian Research Council. IB acknowledges the Australian National Computational Infrastructure Facility and its Western Aus-

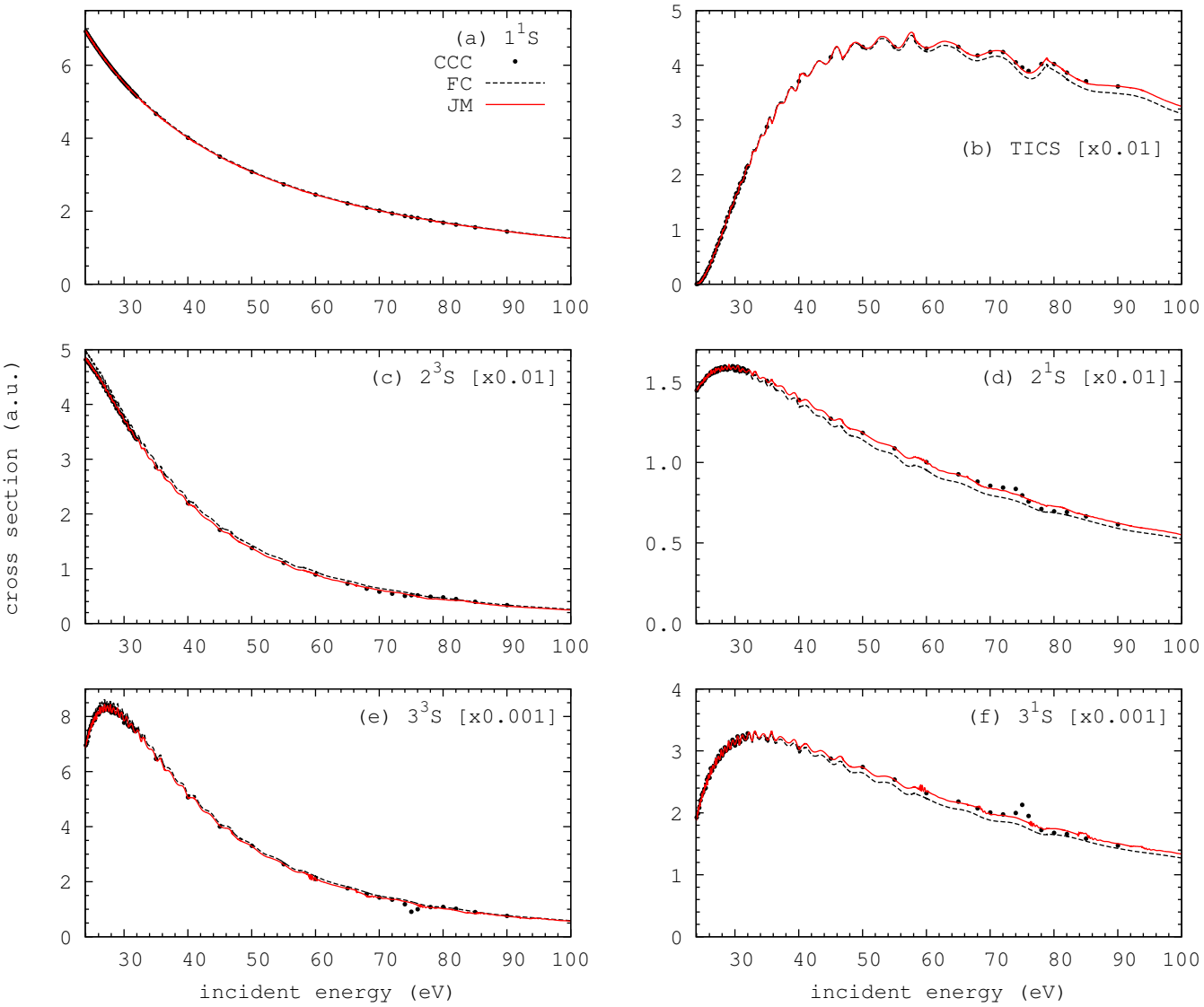

FIG. 4: (Color online) The same as in Fig. 1 but above the ionization threshold.

tralian node iVEC.

[1] A. Temkin, Phys. Rev. **126**, 130 (1962).
[2] E. J. Heller and H. A. Yamani, Phys. Rev. A **9**, 1209 (1974).
[3] R. Poet, J. Phys. B **11**, 3081 (1978).
[4] R. Poet, J. Phys. B **13**, 2995 (1980).
[5] R. Poet, J. Phys. B **14**, 91 (1981).
[6] J. Callaway and D. H. Oza, Phys. Rev. A **29**, 2416 (1984).
[7] I. Bray and A. T. Stelbovics, Phys. Rev. Lett. **69**, 53 (1992).
[8] A. K. Bhatia, B. I. Schneider, and A. Temkin, Phys. Rev. Lett. **70**, 1936 (1993).
[9] D. A. Konovalov and I. E. McCarthy, J. Phys. B **27**, L407 (1994).
[10] W. Ihra, M. Draeger, G. Handke, and H. Friedrich, Phys. Rev. A **52**, 3752 (1995).
[11] M. S. Pindzola and D. R. Schultz, Phys. Rev. A **53**, 1525 (1996).
[12] S. Jones and A. T. Stelbovics, Phys. Rev. A **66**, 032717 (2002).
[13] S. Jones and A. T. Stelbovics, Phys. Rev. Lett. **84**, 1878 (2000).
[14] M. Baertschy, T. N. Rescigno, W. A. Isaacs, and C. W. McCurdy, Phys. Rev. A **60**, R13 (1999).
[15] A. T. Stelbovics, Phys. Rev. Lett. **83**, 1570 (1999).
[16] C. W. McCurdy, D. A. Horner, and T. N. Rescigno, Phys. Rev. A **65**, 042714 (2002).

[17] P. L. Bartlett and A. T. Stelbovics, Phys. Rev. A **69**, 022703 (2004).
[18] A. L. Frapiccini, J. M. Randazzo, G. Gasaneo, and F. D. Colavecchia, J. Phys. B **43**, 101001 (2010).
[19] M. Draeger, G. Handke, W. Ihra, and H. Friedrich, Phys. Rev. A **50**, 3793 (1994).
[20] M. S. Pindzola, D. Mitnik, and F. Robicheaux, Phys. Rev. A **59**, 4390 (1999).
[21] C. Plottke, I. Bray, D. V. Fursa, and A. T. Stelbovics, Phys. Rev. A **65**, 032701 (2002).
[22] C. Plottke, P. Nicol, I. Bray, D. V. Fursa, and A. T. Stelbovics, J. Phys. B **37**, 3711 (2004).
[23] D. A. Horner, C. W. McCurdy, and T. N. Rescigno, Phys. Rev. A **71**, 010701(R) (2005).
[24] D. A. Horner, C. W. McCurdy, and T. N. Rescigno, Phys. Rev. A **71**, 012701 (2005).
[25] P. L. Bartlett and A. T. Stelbovics, Phys. Rev. A **81**, 022715 (2010).
[26] P. L. Bartlett and A. T. Stelbovics, Phys. Rev. A **81**, 022716 (2010).
[27] D. A. Konovalov, D. V. Fursa, and I. Bray, Phys. Rev. A **84**, 032707 (2011).
[28] D. V. Fursa and I. Bray, Phys. Rev. A **52**, 1279 (1995).
[29] W. C. Fon, K. P. Lim, K. Ratnavelu, and P. M. J. Sawey, Phys. Rev. A **50**, 4802 (1994).
[30] M. Stepanovic, M. Minic, D. Cvejanovic, J. Jureta, J. Kurepa, S. Cvejanovic, O. Zatsarinny, and K. Bartschat, J. Phys. B **39**, 1547 (2006).
[31] D. A. Konovalov and I. E. McCarthy, J. Phys. B **27**, L741 (1994).
[32] D. A. Konovalov and I. E. McCarthy, J. Phys. B **28**, L139 (1995).
[33] U. Fano, Phys. Rev. **140**, A67 (1965).
[34] I. Bray and A. T. Stelbovics, Phys. Rev. A **46**, 6995 (1992).
[35] E. J. Heller and H. A. Yamani, Phys. Rev. A **9**, 1201 (1974).
[36] J. Broad and W. Reinhardt, J. Phys. B **9**, 1491 (1976).
[37] *The complete Java source code used in this study is freely available for academic use from jmatrix.googlecode.com or a relevant link at www.dmitrykonovalov.org . .*
[38] D. A. Konovalov and I. Bray, Phys. Rev. A **82**, 022708 (2010).
[39] M. Abramowitz and I. A. Stegun, eds., *Handbook of Mathematical Functions* (Dover Publications, Mineola, NY, 1965).